◆ Human Brain Mapping 36:1705–1715 (2015) ◆

Reorganization of Functional Brain Networks Mediates the Improvement of Cognitive Performance Following Real-Time Neurofeedback Training of Working Memory

Gaoyan Zhang,[1,2] Li Yao,[1,3] Jiahui Shen,[3] Yihong Yang,[4]* and Xiaojie Zhao[1,3]*

[1]*State Key Laboratory of Cognitive Neuroscience and Learning, Beijing Normal University, Beijing 100875, China*
[2]*School of Computer Science and Technology, Tianjin key Laboratory of Cognitive Computing and Application, Tianjin University, Tianjin 300072, China*
[3]*College of Information Science and Technology, Beijing Normal University, Beijing 100875, China*
[4]*Neuroimaging Research Branch, National Institute on Drug Abuse, National Institutes of Health, Baltimore, Maryland 21224*

Abstract: Working memory (WM) is essential for individuals' cognitive functions. Neuroimaging studies indicated that WM fundamentally relied on a frontoparietal working memory network (WMN) and a cinguloparietal default mode network (DMN). Behavioral training studies demonstrated that the two networks can be modulated by WM training. Different from the behavioral training, our recent study used a real-time functional MRI (rtfMRI)-based neurofeedback method to conduct WM training, demonstrating that WM performance can be significantly improved after successfully upregulating the activity of the target region of interest (ROI) in the left dorsolateral prefrontal cortex (Zhang et al., [2013]: PloS One 8:e73735); however, the neural substrate of rtfMRI-based WM training remains unclear. In this work, we assessed the intranetwork and internetwork connectivity changes of WMN and DMN during the training, and their correlations with the change of brain activity in the target ROI as well as with the improvement of post-training behavior. Our analysis revealed an "ROI-network-behavior" correlation relationship underlying the rtfMRI training. Further mediation analysis indicated that the reorganization of functional brain networks mediated the effect of self-regulation of the target brain activity on the improvement of cognitive performance following the neurofeedback training. The results of this study enhance our understanding of the neural basis of real-time neurofeedback and suggest a new direction to improve WM performance by regulating the functional connectivity in the WM related networks. *Hum Brain Mapp 36:1705–1715, 2015.* © 2014 Wiley Periodicals, Inc.

Contract grant sponsor: Funds for International Cooperation and Exchange of the National Natural Science Foundation of China; Contract grant number: 61210001; Contract grant sponsor: National Program on Key Basic Research Project (973 Program); Contract grant number: 2013CB329301; Contract grant sponsor: National Natural Science Foundation of China; Contract grant number: 61473044; Contract grant sponsor: Intramural Research Program of the National Institute on Drug Abuse, National Institutes of Health (to Y.Y.).

*Correspondence to: Xiaojie Zhao, Ph.D., College of Information Science and Technology, Beijing Normal University, Beijing 100875, China. E-mail: zhaoxj86@hotmail.com or Yihong Yang, Ph.D., Neuroimaging Research Branch, National Institute on Drug Abuse, National Institutes of Health, Baltimore, MD 21224. E-mail: yihongyang@mail.nih.gov

Received for publication 4 September 2014; Revised 13 December 2014; Accepted 18 December 2014.

DOI: 10.1002/hbm.22731

Published online 26 December 2014 in Wiley Online Library (wileyonlinelibrary.com).

© 2014 Wiley Periodicals, Inc.

Key words: functional reorganization; working memory network; default mode network; mediation effect; real-time neurofeedback; working memory

INTRODUCTION

Working memory (WM) is essential for a wide range of cognitive tasks, including reading comprehension and problem solving, as well as for academic achievement [Engle and Kane, 2004]. Deficits in WM are considered to be the primary source of cognitive impairment in attention deficit hyperactivity disorder and mathematics disability [Minear and Shah, 2006]. Given the importance of WM, some behavioral training studies have been conducted and the results suggest that WM training is promising for improving individuals' cognitive functions [Klingberg, 2010].

The potential of WM training probably stems from the neuroplasticity of the brain networks underlying the function. WM fundamentally relies on a frontoparietal working memory network (WMN) [Newton et al., 2011; Schlösser et al., 2006] and a cinguloparietal default mode network (DMN) [Buckner et al., 2008]. The WMN mainly includes the dorsolateral prefrontal cortex (DLPFC), premotor area (PMA), supplemental motor area (SMA), and posterior parietal cortex (PPC), whereas the DMN primarily consists of the posterior cingulate cortex (PCC), medial prefrontal cortex (MPFC), inferior parietal cortex (IPC), parahippocampal gyrus (PHG), and middle temporal cortex (MTC). Neural network models suggested that stronger frontoparietal connectivity in the WMN was a potential mechanism underlying higher WM capacity [Edin et al., 2007]. Hampson et al. [2006] provided evidence that functional coupling strength within the resting DMN predicted WM performance. Furthermore, behavioral training studies showed that the resting WMN and DMN connectivity changed as WM performance improved [Jolles et al., 2011; Takeuchi et al., 2012]. Together, these evidences suggest that WM behavior is closely related to the WMN and DMN and that behavioral training could modulate the two networks.

In comparison with the behavioral training approach that used behavior as an independent variable and neural activity as a dependent variable, the real-time functional MRI (rtfMRI)-based neurofeedback method allows manipulation of local brain activity directly, consequently altering the relevant cognitive behaviors [deCharms, 2007]. Recently, a number of studies have demonstrated that cognitive function can be improved by self-control of brain activity in a region of interest (ROI) [Weiskopf, 2012]. Using this neurofeedback approach, our recent study has demonstrated that WM performance was significantly improved after successfully upregulating the left DLPFC activity [Zhang et al., 2013]. However, the neural substrate of rtfMRI training remains unclear. Previous study demonstrated that the principle of neurofeedback training was based on operant learning [Caria et al., 2012], and learning can take place through the efficient use of specific neuronal circuits [Lee et al., 2011]. Thus, the functional interactions among spatially distributed brain areas, and their roles in the behavioral improvement induced by the regulation of local brain activity, need to be explored in depth, which is important to understand where adaptations occur in the human brain during the training and how the brain networks reorganize to optimize the WM function. In the majority of prior rtfMRI studies, effects were mainly reported as increases or decreases of activation in brain areas related to task performance, although some studies provided preliminary evidence that learned control over local brain activity may induce alterations of relevant brain networks [Rota et al., 2011; Ruiz et al., 2011]. However, the neural substrates of WM training remain unknown.

This study aimed to systematically investigate the neural mechanism underlying rtfMRI-based WM training. We assessed the relationship among the signal change in the target ROI (DLPFC), the WMN and DMN connections, and the post-training behaviors. We further conducted a mediation analysis [MacKinnon et al., 2007] to explore the specific role of the WMN and DMN in the rtfMRI training. We hypothesized that (1) self-regulation of left DLPFC activity during rtfMRI would induce reorganization of functional connectivity within and between the WMN and the DMN and that (2) the altered network connections would mediate post-training behavior.

MATERIALS AND METHODS

Subjects

A total of 30 right-handed subjects participated in the study. The experimental group included seven females and eight males (age: 21.47 ± 3.83 years). The other seven females and eight males constituted the control group (age: 21.87 ± 3.41 years). Age and gender were well matched between the two groups. All subjects were free of psychiatric disorders or history of head trauma. Participants signed informed consent forms after the experimental procedures were explained to them prior to scanning and received monetary compensation after the experiment. The study was approved by the Institutional Review Board of the State Key Laboratory of Cognitive Neuroscience and Learning in Beijing Normal University.

Experimental Procedure

The subjects underwent two rtfMRI training sessions (separated by seven days) and a pre- and post-training

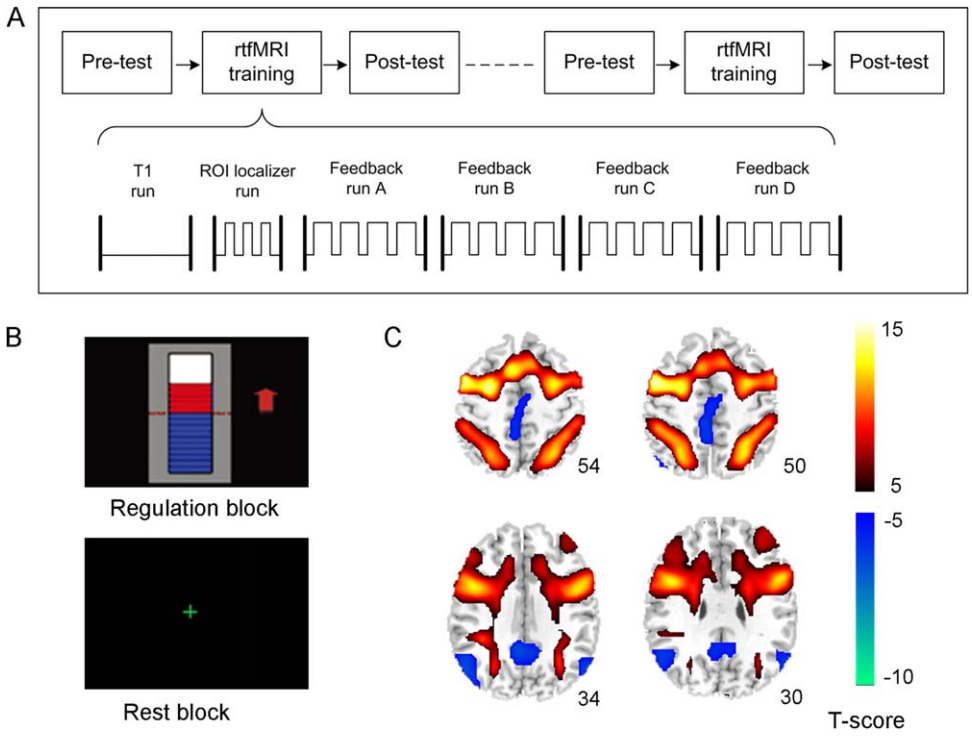

Figure 1.

A. The overall experimental procedure. It included two rtfMRI training sessions and a pre- and post-training behavioral test conducted on the same day before and after each training session. Each rtfMRI training session included a T1 run for functional overlay, an ROI localizer run for definition of feedback ROIs and four feedback training runs. **B.** The feedback information presented in the four feedback runs during the training. **C.** The activation and deactivation maps of the feedback runs of the experimental and control groups together ($P < 0.01$, FDR corrected. Left side is on the reader's left).

behavioral test in each session (Fig. 1A). Each training session included six runs. The first run was a 10-minute T1-weighted imaging which was used for image normalization and functional overlay. In the second run, participants conducted a digital 3-back WM task that reliably activated the target ROI in the left DLPFC. In addition, a control ROI was selected in a task-unrelated area to eliminate unspecific global effects [Zhang et al., 2013]. The subsequent four feedback runs consisted of four regulation blocks (60 s each) alternated with five baseline blocks (30 s each). During the regulation block, the average blood oxygenation level dependent (BOLD) signal change from the target ROI minus the BOLD signal change from the control ROI was presented to the participants in real time as changing bars of a graphical thermometer (Fig. 1B) and subjects were instructed to upregulate their left DLPFC activity as much as possible as guided by the feedback information. The strategy provided to them was to backward recall self-generated digit or letter sequences subvocally, and the length and content of the sequences they generated could be adjusted according to the feedback information. During the resting block, a cross was present to the subjects (Fig. 1B), and they were instructed to relax and rest to return to their baseline-level activity. Because the subjects were instructed to use strategies associated with verbal WM to regulate their BOLD signal in the target ROI, two verbal WM tasks (digit span and letter memory) and two transfer tasks (spatial 3-back and Stroop color-word test) were tested before and after each rtfMRI training session. To verify the training effect, subjects in the control group underwent the same experimental procedure and were given the same instructions, except that they were provided with a sham feedback signal. For more details about the experimental procedure, see our previous study [Zhang et al., 2013].

Scanning Parameter

Brain images were collected using a SIEMENS 3.0 T scanner at the MRI Center of Beijing Normal University. A T1-weighted image of the whole brain was acquired using the following parameters: MPRAGE sequence, matrix = 256 × 256, 176 partitions, 1 mm^3 isotropic voxels, TR = 2530 ms, TE = 3.45 ms, flip angle = 7°. A single-shot T2*-weighted gradient-echo, echo-planar image sequence

was used for the functional imaging acquisition (TR = 2000 ms, TE = 30 ms, matrix = 64 × 64, in-plane resolution = 3.125 × 3.125 mm^2, slice number = 33, slice thickness = 4.0 mm, slice gap = 0.6 mm, flip angle = 90°). To reduce movement, two foam cushions were used to immobilize the participants' heads.

Data Analysis

Network connection analysis

The data used in this study were collected in our previous study [Zhang et al., 2013]. According to Baddeley's multicomponent model [Baddeley, 2003] and previous WMN [Smith et al., 1998] and DMN studies [Greicius et al., 2003], the nodes of the WMN and DMN were selected based on the group activation map obtained by analyzing all the training runs in the two groups together. The fMRI data were first preprocessed in the SPM8 software package (http://www.fil.ion.ucl.ac.uk/spm/), which included the correction of slice acquisition timing, correction of head motion, normalization to Montreal Neurological Institute space, resampling into 3 × 3 × 4 mm^3 voxels, and spatial smoothing using a Gauss kernel with full width at half maximum of 8 mm. Then, the preprocessed data were modeled using a general linear model in which the repressor was constructed by convolving the boxcar function with a canonical hemodynamic response function. After parameter estimation and statistical tests, the individual activation (regulation vs. baseline condition) and deactivation (baseline vs. regulation condition) maps were obtained. One-sample *t*-tests were performed to calculate the group activation and deactivation maps. The statistical threshold was corrected for multiple comparisons using the topological false discovery rate (FDR) [Chumbley and Friston, 2009] at an overall (corrected) alpha level of 0.01. Then, the nodes of the WMN and the DMN were defined as a spherical region centered on the local maximum peak with a radius of 6 mm.

The time series for each of the node ROIs were extracted and the ROI–ROI correlation matrix was computed for each subject in each feedback run. The correlation coefficient was converted to *z*-score using Fisher's transformation [Carbonell et al., 2009]. For each of the ROI–ROI connection pairs, one-way repeated-measure analysis of variance (ANOVA) was conducted with run as the main effect. For all the ROI–ROI connection pairs within a network, the significance of the multiple comparisons was corrected using FDR at an overall (corrected) alpha level of 0.05. The same correction of multiple comparisons was used for the between-network ROI–ROI connection pairs. For the ROI–ROI connection pairs in the WMN survived after the correction, a factor analysis [Lahey et al., 2012] was conducted on their connection strengths to extract a WMN connection factor. The logic behind the factor analysis was to search for a common connection strength at the network level. The factor loadings represented the degree to which each of the survived ROI–ROI connection pairs correlates with the WMN connection factor. The similar factor analyses were performed on the survived ROI–ROI connection pairs in the DMN and between the WMN and DMN (WMN–DMN). Comparison of factor scores in run D of second training session (2nd_D) with that in run A of first training session (1st_A) was conducted to evaluate the alteration of internetwork and intranetwork connection strength.

Correlation of network connections with BOLD signal in the target ROI and with behavior

Pearson correlations of the change of the BOLD signal intensity in the target ROI (run 2nd_D vs. run 1st_A) with the change of the WMN, DMN, and WMN–DMN connection factors (run 2nd_D vs. run 1st_A) were computed, respectively, to evaluate how the self-regulation of target brain activity affected the brain networks. To investigate the relationship between the network connections and post-training behavior, Pearson correlations of the change of the three network connection factors (run 2nd_D vs. run 1st_A) with the change of behavioral performance in the post-test after the second training session (2nd post-test) compared with that in the pre-test of first training session (1st pre-test) were conducted. The behavioral performance included the verbal WM performance assessed by factor analysis of the changes in digit span and letter memory performance, dprime of the spatial 3-back task (3B-dprime) estimated by the hit rate penalized by the false alarm rate [Haatveit et al., 2010], response time of the spatial 3-back task (3B-RT), and response time of the Stroop color-word test (Stroop-RT).

Mediation analysis

To determine whether the behavioral improvement potentially induced by the self-regulation of the target brain activity was mediated by the brain network connections, a mediation analysis model was constructed using the structural equation modeling method [Boucard et al., 2007] in AMOS 17.0 (SPSS, Chicago, IL). The changes of WMN connection factor, DMN connection factor, and WMN–DMN connection factor between run 2nd_D and run 1st_A were selected as three mediators. The change of BOLD signal intensity in the target ROI (run 2nd_D vs. run 1st_A) and the change of the four behavioral indexes (2nd post-test vs. 1st pre-test), that is, verbal WM performance, 3B-dprime, 3B-RT, and Stroop-RT, were included in the model. The mediation model was estimated using the maximum likelihood algorithm and statistically tested using a Chi-square test. The mediation effect of each mediator on each behavioral index was evaluated using the Sobel test [Sobel, 1982].

RESULTS

Determination of the Nodes in the WMN and DMN

The activation and deactivation maps of the two groups together are shown in Figure 1C. Based on this result, we

TABLE I. The location of the node ROIs in each network (WMN: working memory network; DMN: default mode network)

Node ROIs	Side	Brodmann's area	MNI coordinates			Peak *T*-score
			x	*y*	*z*	
WMN						
Supplement motor area	Left	6	−3	11	54	13.93
Premotor area	Left	6	−27	−1	50	13.60
Premotor area	Right	6	30	−1	50	12.71
Posterior parietal cortex	Right	7	30	−61	50	12.43
Posterior parietal cortex	Left	7	−27	−64	50	11.71
Inferior frontal gyrus	Left	44	−51	11	10	8.14
Dorsal lateral prefrontal cortex	Left	9	−45	29	34	7.10
Dorsal lateral prefrontal cortex	Right	9	42	35	34	5.40
DMN						
Medial prefrontal cortex	Left	32	−3	35	−10	−7.93
Inferior parietal cortex	Left	39	−51	−67	30	−7.67
Posterior cingulate cortex	Left	31	−6	−49	30	−7.45
Inferior parietal cortex	Right	39	51	−67	30	−7.27
Middle temporal cortex	Left	21	−60	−22	−18	−5.15
Parahippocampal gyrus	Left	35	−18	−10	−26	−4.40
Middle temporal cortex	Right	21	57	−7	−18	−3.75
Parahippocampal gyrus	Right	35	21	−10	−26	−3.70

selected the bilateral DLPFC, bilateral PPC, bilateral PMA, SMA, and Broca's area (left inferior frontal gyrus, L.IFG) as the nodes of the WMN and the PCC, MPFC, bilateral IPC, bilateral MTC, and bilateral PHG as the nodes of the DMN (Fig. 1C). The local maximum peaks of these regions are listed in Table I.

Training-Induced Changes of Within- and Between-Network Connections

In the experimental group, one-way ANOVA of the ROI–ROI connection pairs in the WMN showed that the connection strengths of L.DLPFC-R.DLPFC, L.DLPFC-R.PPC, R.DLPFC-R.PPC, R.DLPFC-L.PMA, L.PMA-R.PMA, and L.PMA-L.PPC showed significant main effect of run (L. and R. mean left and right side, $P < 0.05$, FDR correction, Fig. 2A). Post hoc analysis demonstrated that these connection strengths were significantly increased during the training. One WMN connection factor was extracted through factor analysis of these six connection pairs (Kaiser–Meyer–Olkin, KMO value is 0.759, the significance of Bartlett's test of sphericity is $P < 0.001$) and the factor loadings were 0.187, 0.233, 0.184, 0.251, 0.217, and 0.209, respectively, for the six connections. The WMN connection factor showed a significant linear increasing trend (linear regression analysis, $R^2 = 0.774$, $P < 0.0001$) across training runs. Paired *t*-test showed that there was a significant difference in the WMN connection factor between run 2nd_D and run 1st_A with $P = 0.03$ (Fig. 2B).

A similar analysis in the DMN indicated that the connection strengths of PCC-L.PHG, PCC-R.PHG, and PCC-L.MTC showed significant main effect of run and their connection strengths were significantly increased during the training ($P < 0.05$, FDR correction, Fig. 2A). There was one DMN connection factor extracted by factor analysis of the three ROI–ROI connection pairs (KMO = 0.698, the significance of Bartlett's test of sphericity is $P < 0.001$) and the factor loadings were 0.394, 0.382, and 0.357, respectively, for the three connection pairs. The DMN connection factor exhibited a significant increasing trend (linear regression analysis, $R^2 = 0.861$, $P < 0.0001$) across training runs. Comparison of run 1st_A with run 2nd_D demonstrated a significant difference in the DMN connection factor ($P = 0.0017$, paired *t*-test, Fig. 2C).

One-way ANOVA for the between-network connections demonstrated that the connection strengths of L.IFG-L.PHG, L.IFG-R.PHG, L.PMA-L.PHG, L.PMA-R.PHG, SMA-L.PHG, SMA-R.PHG, R.PPC-L.PHG, R.PPC-R.PHG, R.DLPFC-R.PHG, L.PPC-R.PHG, L.PMA-PCC, L.DLPFC-R.PHG, and R.PMA-R.PHG showed significant main effect of run ($P < 0.05$, FDR correction, Fig. 2A). Post hoc analysis revealed that these connection strengths were significantly increased during the training. Factor analysis showed that one WMN–DMN connection factor was extracted from these ROI–ROI connections (KMO = 0.845, the significance of Bartlett's test of sphericity is $P < 0.001$) and the factor loading were 0.090, 0.095, 0.096, 0.099, 0.087, 0.098, 0.089, 0.095, 0.092, 0.096, 0.077, 0.089, and 0.079, respectively, for these connections. Moreover, the WMN–DMN connection factor increased linearly across training runs (linear regression analysis, $R^2 = 0.915$, $P < 0.0001$). There was a significant difference in the WMN–DMN connection factor in the comparison of run 1st_A with run 2nd_D ($P = 0.0001$, paired *t*-test, Fig. 2D).

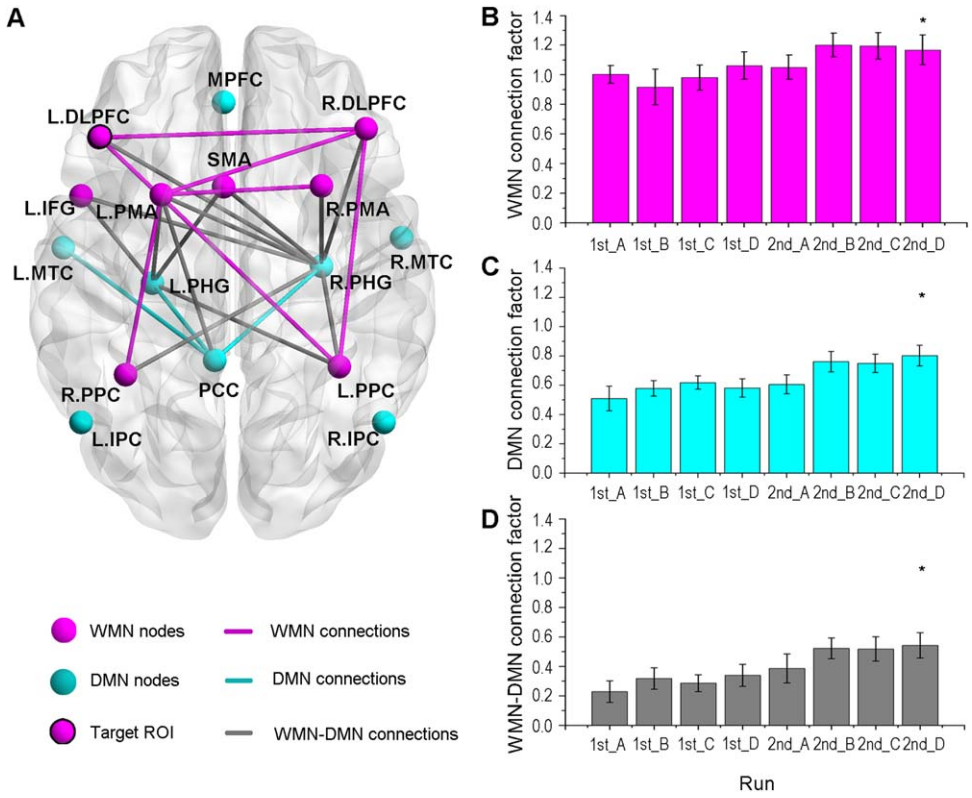

Figure 2.

The change of network connections during the two sessions of rtfMRI training. **A.** The significantly changed within- and between-network ROI–ROI connections ($P < 0.05$, FDR corrected, the L. and R. refer to the left and right side, respectively). **B.** The change of the WMN connection factor across feedback runs. **C.** The change of the DMN connection factor across feedback runs. **D.** The change of the WMN–DMN connection factor across feedback runs. The three factors were calculated by factor analysis of the significantly changed within- and between-network ROI–ROI connections in all eight runs, respectively. * refers to significant difference ($P < 0.05$) in the comparison of run 2nd_D with run 1st_A.

For the control group, no significant alterations of within- or between-network connections were observed after FDR correction; therefore, the following analysis was conducted only in the experimental group.

Correlation of Network Connections With BOLD Signal in the Target ROI and With Behavior

The BOLD signal in the target ROI showed a positive correlation with the WMN connection factor ($r = 0.65$, $P = 0.004$, Fig. 3A), but not with the DMN connection factor or with the WMN–DMN connection factor (Table II).

The WMN connection factor showed a negative correlation with the 3B-RT ($r = -0.50$, $P = 0.029$, Fig. 3B). The DMN connection factor and the WMN–DMN connection factor exhibited significant correlations with verbal WM performance ($r = 0.45$, $P = 0.046$, Fig. 3C and $r = 0.57$, $P = 0.013$, Fig. 3D, respectively).

Mediation Effect of the Network Connections

Mediation effect analysis was conducted to directly assess the role of the WMN and DMN in rtfMRI-based WM training. A successful mediation model was identified (Chi-square = 10.799, degrees of freedom = 9, $P = 0.29$, comparative fit index = 0.907, Fig. 4 and Table III).

The path analysis demonstrated a significant impact of target ROI on WMN connection factor (path coefficient = 0.651, $P = 0.001$) and a significant effect of WMN connection factor on verbal WM performance (path coefficient = 0.705, $P < 0.001$). Mediation effect analysis showed that the influence of target ROI on verbal WM performance was mediated by the WMN connection factor (mediation effect = 0.52, $P = 0.01$, two-tail Sobel test). The path coefficient from the WMN connection factor to the 3B-RT was also significant (path coefficient = −0.739, $P = 0.011$), and the mediation analysis indicated that the effect of target ROI on the 3B-RT was also mediated by the WMN connection factor (mediation effect = −0.455, $P = 0.02$, two-

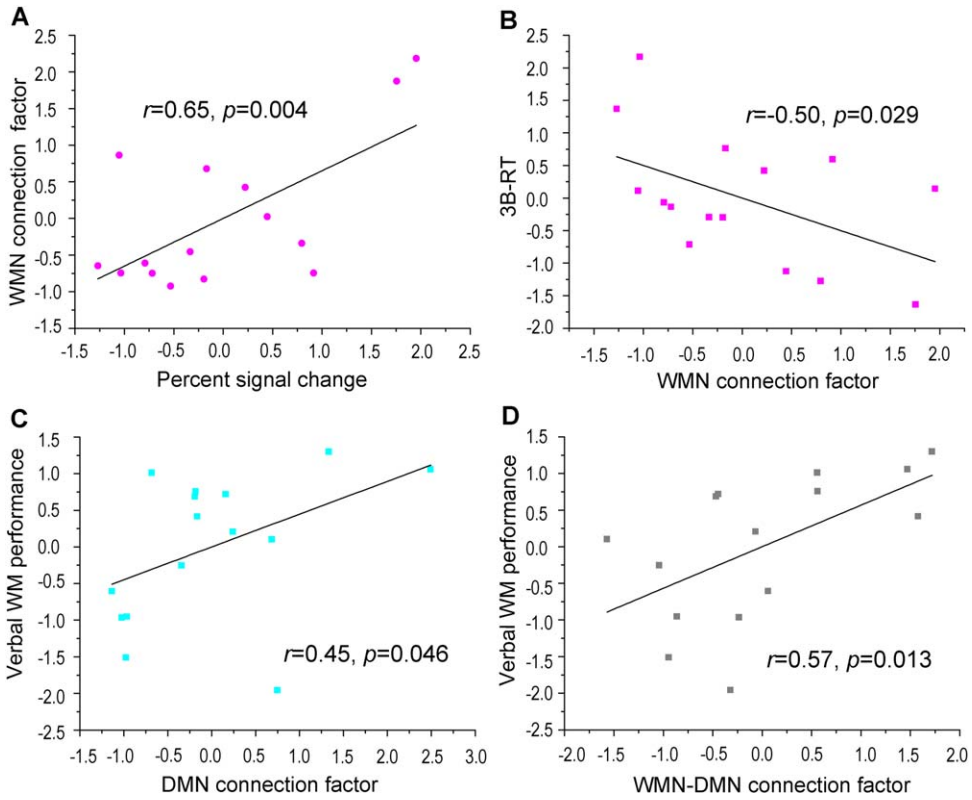

Figure 3.

The correlation of network connection factors with the percent signal change of the target ROI and with the behaviors. **A.** The positive correlation of percent signal change in the target ROI with the WMN connection factor. **B.** The negative correlation of the WMN connection factor with the response time of the spatial 3-back task. **C.** The positive correlation of the DMN connection factor with verbal WM performance. **D.** The positive correlation of the WMN–DMN connection factor with verbal WM performance. The data shown in the scatter plot were normalized. [Color figure can be viewed in the online issue, which is available at wileyonlinelibrary.com.]

tail Sobel test). Moreover, path analysis demonstrated a significant effect of the WMN–DMN connection factor on the 3B-dprime (path coefficient = 0.491, $P = 0.03$) and on the Stroop-RT (path coefficient = −0.480, $P = 0.041$), but there were no mediation effects detected for the WMN–DMN connection factor on these two behaviors.

DISCUSSION

This study explored the change of functional connectivity within and between the WMN and DMN during the neurofeedback training and their correlations with the alteration of brain activity in the target ROI, as well as with the improvement of post-training behaviors, aiming

TABLE II. The correlations of the WMN connection factor, DMN connection factor, and WMN–DMN connection factor with the alteration of signal in the target region of the left DLPFC and with the change of the four behavioral indexes (the correlation coefficient with * means $P < 0.05$)

Network connection factors	Correlation with BOLD signal change	Correlation with behavioral performance			
		Verbal WM	3B-dprime	3B-RT	Stroop-RT
WMN	0.65*	0.36	−0.24	−0.50*	−0.16
DMN	0.10	0.45*	−0.03	−0.16	0.09
WMN–DMN	−0.02	0.57*	0.36	0.02	−0.34

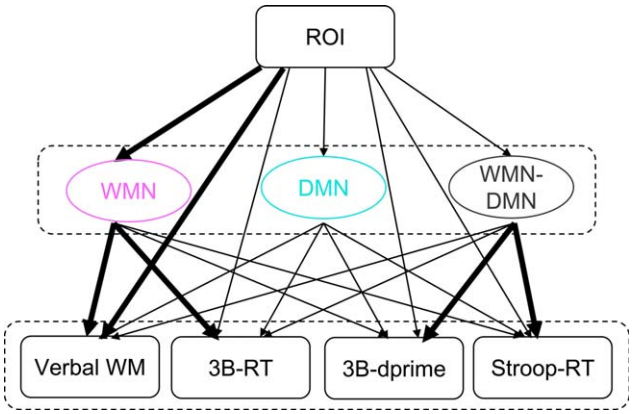

Figure 4.

The mediation effect analysis of the WMN connection factor, DMN connection factor, and WMN–DMN connection factor in the "ROI-network-behavior" model (the bold arrows represent significant path coefficients, $P < 0.05$; the mediation effect of WMN connection factor on verbal WM performance is 0.52, $P = 0.01$, two-tail Sobel test; the mediation effect of WMN connection factor on the response time of spatial 3-back (3B-RT) task is −0.455, $P = 0.02$, two-tail Sobel test). [Color figure can be viewed in the online issue, which is available at wileyonlinelibrary.com.]

to investigate the neurobiological mechanisms of rtfMRI-based WM training. Results showed that self-regulation of the activation in a key region of the WMN induced changes in network connections, which seemed to result in relevant behavioral improvements. Further mediation analysis demonstrated the mediation role of brain networks in rtfMRI-based WM training.

Recruitment of the WMN and DMN in rtfMRI Training

During the rtfMRI training, regions in the WMN and the DMN were significantly activated and deactivated, respectively, (Fig. 1C) and the detected network nodes were in line with previous WMN [Newman et al., 2002a] and DMN [Buckner et al., 2008] studies. These results suggested that the two networks were recruited in the rtfMRI-based WM training and were closely associated with WM functioning.

Changes of WMN Connections

The six functional connection pairs that showed increased connection strengths in the WMN were observed among the nodes in the DLPFC, PPC, and PMA (Fig. 2A). Neuroimaging studies of WM have demonstrated that the DLPFC is involved in allocating the attentional resources for task-relevant stimuli or responses, so as to select and manage (e.g., update) the information to be rehearsed [Curtis and D'Esposito, 2003]. A verbal WM study indicated that the DLPFC–PMA connection was important for articulatory rehearsal [Koechlin et al., 2003]. Also, the functional interactions between frontal and parietal regions play a key role in the maintenance of WM information [Newman et al., 2002b]. A previous study pointed out that synchrony of neural activity may increase the effectiveness of inter-regional connections and enhance the representation of attended stimuli [Buschman and Miller, 2007]. Therefore, the increased functional coupling in the WMN suggested an increased efficiency for information rehearsal and maintenance during the training. Moreover, factor analysis of these ROI–ROI connection pairs in the WMN showed a linearly increasing trend across feedback runs (Fig. 2B). Because subjects reported that they used a strategy of gradually increasing the difficulty of backward recall to regulate the brain activity [Zhang et al., 2013], this finding implies that the WMN connections were memory load dependent, which has been reported in some prior studies [Honey et al., 2002; Newton et al., 2011; Schlösser et al., 2006]. The same trend in the DMN connection factor (Fig. 2C) and the WMN–DMN connection factor (Fig. 2D) may also suggest the load effect. Interestingly, the increase of WMN connection was positively correlated with the increase of BOLD signal change in the target ROI of the left DLPFC (Fig. 3A). This outcome is consistent with the previous finding that self-regulation of local brain activity can alter the functional connectivity of the relevant network [Rota et al., 2011]. The connection-behavior correlations showed that the increase in WMN connection was significantly correlated with the decrease in 3B-RT (Fig. 3B), suggesting that the increased WMN connections modulated post-training behavior.

TABLE III. The estimation of the path coefficient and its significance (S.E. means standard error; C.R. means critical ratio; the *P* values less than 0.05 were marked with*)

Paths	Estimate	S.E.	C.R.	*P* value
ROI → WMN	0.651	0.203	3.207	0.001*
ROI → WMN–DMN	−0.025	0.267	−0.093	0.926
ROI → DMN	0.096	0.266	0.362	0.717
ROI → stroop-RT	−0.163	0.310	−0.524	0.600
ROI → verbal WM	−0.725	0.206	−3.522	<0.0001*
WMN → stroop-RT	−0.049	0.309	−0.160	0.873
ROI → 3B-RT	0.248	0.310	−0.524	0.600
WMN → 3B-RT	−0.739	0.291	−2.534	0.011*
WMN–DMN → 3B-RT	0.241	0.221	1.088	0.277
ROI → 3B-dprime	−0.137	0.299	−0.460	0.645
WMN → 3B-dprime	−0.241	0.298	−0.809	0.418
WMN–DMN → 3B-dprime	0.491	0.226	2.172	0.030*
WMN–DMN → verbal WM	0.297	0.156	1.907	0.056
DMN → 3B-dprime	−0.135	0.227	−0.593	0.553
DMN → 3B-RT	0.014	0.222	0.061	0.951
DMN → stroop-RT	0.342	0.246	1.450	0.147
DMN → verbal WM	0.099	0.157	0.635	0.525
WMN → verbal WM	0.705	0.205	3.436	<0.001*
WMN–DMN → stroop-RT	−0.480	0.235	−2.044	0.041*

Changes of DMN Connections

In the DMN, ROI–ROI connection pairs that showed increased functional connectivity were found in the PCC-L.MTC, PCC-L.PHG, and PCC-R.PHG (Fig. 2A). The consistent increases of connections with the PCC were coincident with a previous study that revealed that the PCC node in the DMN acted as a convergence node where information processing in the other nodes in the DMN was integrated [Fransson and Marrelec, 2008]. It has been shown that the MTC is involved in semantic processing [Hoffman et al., 2012]. An fMRI study of a delayed match-to-sample task revealed that sustained activity in the PHG may underlie long-term encoding as well as active maintenance of novel information during the brief memory delay [Ranganath and D'Esposito, 2001; Stern et al., 2001]. The PCC was thought to contribute to the transition from short to long-term memory by playing a direct role in output monitoring, encoding or retrieval strategies [Kobayashi and Amaral, 2003]. A study of monkey anatomy suggested that the PCC was heavily connected with the PHG, receiving nearly 40% of its extrinsic input from the medial temporal lobe (including PHG and hippocampal formation) and the PCC also projected back to the medial temporal lobe [Kobayashi and Amaral, 2003]. A study of human beings demonstrated reduced functional connectivity of the PCC with the medial temporal lobe and with the MTC in patients with amnesic mild cognitive impairment, a syndrome with a high risk of developing into Alzheimer's disease [Bai et al., 2009; Sorg et al., 2007]. These studies suggest that the PCC–PHG and PCC–MTC connections in the DMN are important for memory function. The significant correlation of DMN connection with verbal WM performance (Fig. 3C) further provides evidence that the DMN plays a pivotal role in the process of WM information.

Changes of WMN–DMN Connections

Between-network connection analysis indicated that the functional connectivity of frontoparietal areas in the WMN with the PCC as well as with the PHG in the DMN was significantly increased during the training (Fig. 2A) and a significant correlation of the WMN–DMN connection with verbal WM performance was observed (Fig. 3D). The increases of connectivity between the PCC and the WMN nodes are consistent with a role for this region in modulating the dynamic interaction between these two networks controlling the efficient allocation of attention [Leech et al., 2011]. With respect to the PHG, a single unit recording study indicated that the prefrontal cortex exerted top-down control upon the PHG in memory retrieval [Tomita et al., 1999]. A study of the N-back paradigm showed that interaction between the PPC and the PHG was related to the different strategies used by the individuals to perform the WM task [Glabus et al., 2003]. Moreover, a recent study demonstrates that the prefrontal and parietal regions

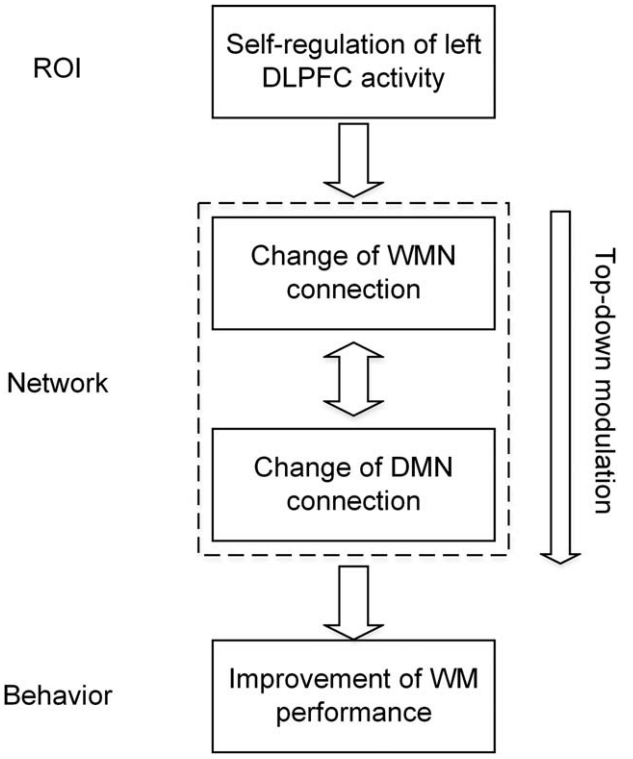

Figure 5.
The "ROI-network-behavior" relationship underlying the rtfMRI training.

are the sources of a top-down signal that exert top-down control upon the sensory cortex, even in the absence of WM stimuli [Gazzaley and Nobre, 2012]. Therefore, the increased between-network functional interaction may imply top-down modulation during the rtfMRI training, which resulted in an efficient allocation of attention and strategy to active selection and retrieval of the memory information necessary for the WM training and an inhibition of the interfering information, such that relevant representations can be effectively used to guide behavior (Fig. 5).

Mediation Effects of the Network Connections in the Impact of the Target ROI on the Behaviors

The above analysis implied that intentional regulation of the percent signal change in the target ROI through rtfMRI induced the change of WMN connections, the functional interaction between the WMN and DMN led to the change of connections in the DMN, and these altered network connections subsequently modulated the post-training WM performance. Therefore, there may exist a "ROI-network-behavior" relationship in the rtfMRI training (Fig. 5); that is, the WMN and DMN may act as mediators between the signal change in the target ROI and verbal

WM as well as transfer behaviors. To clarify this hypothesis, this study conducted a mediation analysis. The result provided evidence that the WMN connection factor acted as a mediator of the effect of the BOLD signal change in the target ROI on the improvement of verbal WM performance as well as on the change of 3B-RT, but no mediation effects of WMN connection were observed for the 3B-dprime or for the Stroop-RT (Fig. 4). With respect to the DMN connection factor and the WMN–DMN connection factor, there were no mediation effects on verbal WM or the transfer tasks, but significant path coefficients between the WMN–DMN connections and the performances of transfer tasks were detected (Table III), suggesting that the performance of transfer WM tasks was modulated by the intranetwork functional interaction. This result also provided direct evidence for the previous finding that the connection between the WMN and DMN can predict WM performance [Sala-Llonch et al., 2012]. The different role of network connections in the modulation of the four behavioral indexes suggested that there might be different neural bases underlying the improvement of the trained and the transferred behaviors in the experimental group. For the control group, although the transfer task performances were also improved [Zhang et al., 2013], no significant changes in network connections were observed during the rtfMRI training. Because the difference between the two groups was the neurofeedback information, the different extent of recruitment of the brain networks during the rtfMRI training in the two groups may reflect the neural basis of neurofeedback.

SUMMARY

Taken together, based on the fundamental assumption that the brain operates as a system where spatially distributed brain areas interact with each other, this study provides evidence for brain network reorganization at the system level due to the self-regulation of target ROI activation, and revealed their specific roles in the modulation of post-training behavior. The differential changes in the functional networks between the experimental and control group during training and the differential modulation mechanisms for the verbal WM task and the transfer tasks in the experimental group enhance our understanding of the neural substrate underlying real-time neurofeedback training. Moreover, this study demonstrates the neuroplasticity of the WMN and DMN, thus providing a new direction to improve WM performance by regulating the functional connectivity in the WM-related networks.

ACKNOWLEDGMENTS

We declare that we have no actual or potential conflict of interest including any financial, personal or other relationships with other people or organizations that can inappropriately influence our work.

REFERENCES

Baddeley A (2003): Working memory: Looking back and looking forward. Nat Rev Neurosci 4:829–839.

Bai F, Watson DR, Yu H, Shi Y, Yuan Y, Zhang Z (2009): Abnormal resting-state functional connectivity of posterior cingulate cortex in amnestic type mild cognitive impairment. Brain Res 1302:167–174.

Boucard A, Marchand A, Nogues X (2007): Reliability and validity of structural equation modeling applied to neuroimaging data: A simulation study. J Neurosci Methods 166:278–292.

Buckner R, Andrews-Hanna J, Schacter D (2008): The brain's default network. Ann N Y Acad Sci 1124:1–38.

Buschman TJ, Miller EK (2007): Top-down versus bottom-up control of attention in the prefrontal and posterior parietal cortices. Science 315:1860–1862.

Carbonell F, Worsley KJ, Trujillo-Barreto NJ (2009): On the Fisher's transformation of correlation random fields. Stat Probabil Lett 79:780–788.

Caria A, Sitaram R, Birbaumer N (2012): Real-time fMRI a tool for local brain regulation. Neuroscientist 18:487–501.

Chumbley JR, Friston KJ (2009): False discovery rate revisited: FDR and topological inference using Gaussian random fields. Neuroimage 44:62–70.

Curtis CE, D'Esposito M (2003): Persistent activity in the prefrontal cortex during working memory. Trends Cogn Sci 7:415–423.

deCharms RC (2007): Reading and controlling human brain activation using real-time functional magnetic resonance imaging. Trends Cogn Sci 11:473–481.

Edin F, Macoveanu J, Olesen P, Tegnér J, Klingberg T (2007): Stronger synaptic connectivity as a mechanism behind development of working memory-related brain activity during childhood. J Cogn Neurosci 19:750–760.

Engle RW, Kane MJ (2004): Executive attention, working memory capacity, and a two-factor theory of cognitive control. Psychol Learn Motiv 44:145–200.

Fransson P, Marrelec G (2008): The precuneus/posterior cingulate cortex plays a pivotal role in the default mode network: Evidence from a partial correlation network analysis. Neuroimage 42:1178–1184.

Gazzaley A, Nobre AC (2012): Top-down modulation: Bridging selective attention and working memory. Trends Cogn Sci 16: 129–135.

Glabus MF, Horwitz B, Holt JL, Kohn PD, Gerton BK, Callicott JH, Meyer-Lindenberg A, Berman KF (2003): Interindividual differences in functional interactions among prefrontal, parietal and parahippocampal regions during working memory. Cereb Cortex 13:1352–1361.

Greicius MD, Krasnow B, Reiss AL, Menon V (2003): Functional connectivity in the resting brain: A network analysis of the default mode hypothesis. Proc Natl Acad Sci USA 100:253–258.

Haatveit BC, Sundet K, Hugdahl K, Ueland T, Melle I, Andreassen OA (2010): The validity of d prime as a working memory index: Results from the "Bergen n-back task." J Clin Exp Neuropsyc 32:871–880.

Hampson M, Driesen NR, Skudlarski P, Gore JC, Constable RT (2006): Brain connectivity related to working memory performance. J Neurosci 26:13338–13343.

Hoffman P, Pobric G, Drakesmith M, Lambon Ralph MA (2012): Posterior middle temporal gyrus is involved in verbal and non-verbal semantic cognition: Evidence from rTMS. Aphasiology 26:1119–1130.

Honey G, Fu C, Kim J, Brammer M, Croudace T, Suckling J, Pich E, Williams S, Bullmore E (2002): Effects of verbal working memory load on corticocortical connectivity modeled by path analysis of functional magnetic resonance imaging data. Neuroimage 17:573–582.

Jolles DD, van Buchem MA, Crone EA, Rombouts SA (2011): Functional brain connectivity at rest changes after working memory training. Hum Brain Mapp 34:6–406.

Klingberg T (2010): Training and plasticity of working memory. Trends Cogn Sci 14:317–324.

Kobayashi Y, Amaral DG (2003): Macaque monkey retrosplenial cortex: II. Cortical afferents. J Comp Neurol 466:48–79.

Koechlin E, Ody C, Kouneiher F (2003): The architecture of cognitive control in the human prefrontal cortex. Science 302:1181–1185.

Lahey BB, McNealy K, Knodt A, Zald DH, Sporns O, Manuck SB, Flory JD, Applegate B, Rathouz PJ, Hariri AR (2012): Using confirmatory factor analysis to measure contemporaneous activation of defined neuronal networks in functional magnetic resonance imaging. Neuroimage 60:1982–1991.

Lee S, Ruiz S, Caria A, Veit R, Birbaumer N, Sitaram R (2011): Detection of Cerebral Reorganization Induced by Real-Time fMRI Feedback Training of Insula Activation A Multivariate Investigation. Neurorehabil Neural Repair 25:259–267.

Leech R, Kamourieh S, Beckmann CF, Sharp DJ (2011): Fractionating the default mode network: Distinct contributions of the ventral and dorsal posterior cingulate cortex to cognitive control. J Neurosci 31:3217–3224.

MacKinnon DP, Fairchild AJ, Fritz MS (2007): Mediation analysis. Annu Rev Psychol 58:593–614.

Minear M, Shah P (2006): Educational Psychology. In: Working Memory and Education. New York: Academic Press. pp 273–307.

Newman SD, Just MA, Carpenter PA (2002a): Synchronization of the human cortical working memory network. Neuroimage 15: 810–822.

Newman SD, Just MA, Carpenter PA (2002b): Synchronization of the human cortical working memory network. Neuroimage 15: 810–822.

Newton AT, Morgan VL, Rogers BP, Gore JC (2011): Modulation of steady state functional connectivity in the default mode and working memory networks by cognitive load. Hum Brain Mapp 32:1649–1659.

Ranganath C, D'Esposito M (2001): Medial temporal lobe activity associated with active maintenance of novel information. Neuron 31:865–873.

Rota G, Handjaras G, Sitaram R, Birbaumer N, Dogil G (2011): Reorganization of functional and effective connectivity during real-time fMRI-BCI modulation of prosody processing. Brain Lang 117:123–132.

Ruiz S, Lee S, Soekadar SR, Caria A, Veit R, Kircher T, Birbaumer N, Sitaram R. (2011): Acquired self?control of insula cortex modulates emotion recognition and brain network connectivity in schizophrenia. Hum Brain Mapp 34:200–212.

Sala-Llonch R, Pena-Gomez C, Arenaza-Urquijo EM, Vidal-Piñeiro D, Bargallo N, Junque C, Bartres-Faz D (2012): Brain connectivity during resting state and subsequent working memory task predicts behavioural performance. Cortex 48:1187–1196.

Schlösser R, Wagner G, Sauer H (2006): Assessing the working memory network: Studies with functional magnetic resonance imaging and structural equation modeling. Neuroscience 139:91–103.

Smith EE, Jonides J, Marshuetz C, Koeppe RA (1998): Components of verbal working memory: Evidence from neuroimaging. Proc Natl Acad Sci USA 95:876–882.

Sobel ME (1982): Asymptotic confidence intervals for indirect effects in structural equation models. In: Leinhardt S, editor. Sociological Methodology. Washington DC: American Sociological Association. pp 290–312.

Sorg C, Riedl V, Mühlau M, Calhoun VD, Eichele T, Läer L, Drzezga A, Förstl H, Kurz A, Zimmer C (2007): Selective changes of resting-state networks in individuals at risk for Alzheimer's disease. Proc Natl Acad Sci USA 104:18760–18765.

Stern CE, Sherman SJ, Kirchhoff BA, Hasselmo ME (2001): Medial temporal and prefrontal contributions to working memory tasks with novel and familiar stimuli. Hippocampus 11:337–346.

Takeuchi H, Taki Y, Nouchi R, Hashizume H, Sekiguchi A, Kotozaki Y, Nakagawa S, Miyauchi CM, Sassa Y, Kawashima R (2012): Effects of working memory-training on functional connectivity and cerebral blood flow during rest. Cortex 49: 2106–2125.

Tomita H, Ohbayashi M, Nakahara K, Hasegawa I, Miyashita Y (1999): Top-down signal from prefrontal cortex in executive control of memory retrieval. Nature 401:699–703.

Weiskopf N (2012): Real-time fMRI and its application to neurofeedback. Neuroimage 62:682–692.

Zhang G, Yao L, Zhang H, Long Z, Zhao X (2013): Improved working memory performance through self-regulation of dorsal lateral prefrontal cortex activation using real-time fMRI. PloS One 8:e73735.